Monoclonal Antibody-Functionalized Multilayered Particles: Targeting Cancer Cells in the Presence of Protein Coronas

Qiong Dai,[†] Yan Yan,[†] Ching-Seng Ang,[‡] Kristian Kempe,[†] Marloes M. J. Kamphuis,[†] Sarah J. Dodds,[†] and Frank Caruso*[,†]

[†]ARC Centre of Excellence in Convergent Bio-Nano Science and Technology and the Department of Chemical and Biomolecular Engineering, The University of Melbourne, Parkville, Victoria 3010, Australia and [‡]Bio21 Molecular Science and Biotechnology Institute, The University of Melbourne, Parkville, Victoria 3010, Australia

ABSTRACT Engineered particles adsorb biomolecules (*e.g.*, proteins) when introduced in a biological medium to form a layer called a "corona". Coronas, in particular the protein corona, play an important role in determining the surface properties of particles and their targeting abilities. This study examines the influence of protein coronas on the targeting ability of layer-by-layer (LbL)-assembled polymer capsules and core–shell particles functionalized with monoclonal antibodies. Upon exposure of humanized A33 monoclonal antibody (huA33 mAb)-functionalized poly(methacrylic acid) (PMA) capsules or huA33 mAb-PMA particles to human serum, a total of 83 or 65 proteins were identified in the protein coronas, respectively. Human serum of varying concentrations altered the composition of the protein corona. The antibody-driven specific cell membrane binding was qualitatively and quantitatively assessed by flow cytometry and fluorescence microscopy in both the absence and presence of a protein corona. The findings show that although different protein coronas formed in human serum (at different concentrations), the targeting ability of both the huA33 mAb-functionalized PMA capsules and particles toward human colon cancer cells was retained, demonstrating no significant difference compared with capsules and particles in the absence of protein coronas: ~70% and ~90% A33-expressing cells were targeted by the huA33 mAb-PMA capsules and particles, respectively, in a mixed cell population. This result demonstrates that the formation of protein coronas did not significantly influence the targeting ability of antibody-functionalized LbL-polymer carriers, indicating that the surface functionality of engineered particles in the presence of protein coronas can be preserved.

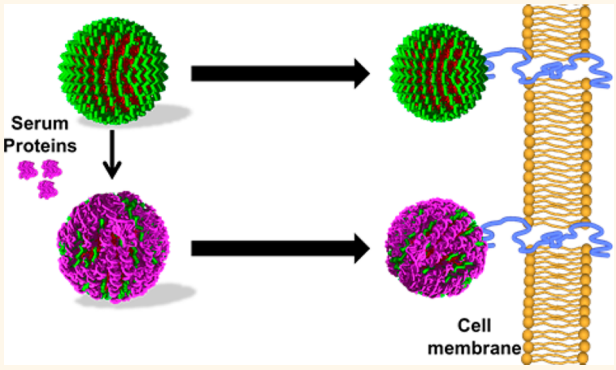

KEYWORDS: protein corona · targeted drug delivery · monoclonal antibody · polymer particles · layer-by-layer assembly · human serum

Engineering targeted drug delivery systems that can accumulate at specific types of cells or tissues to enhance drug efficacy is of widespread interest.[1−4] Discoveries in the biomedical science area have led to the development of a spectrum of targeting molecules including folic acid,[5] transferrin,[6] aptamers,[7] peptides,[8] and a series of specific monoclonal antibodies (mAbs).[9] Consequently, using targeting molecules to functionalize drug carriers to improve their specificity has become a widely used strategy. For example, anti-CD105 monoclonal antibodies were conjugated to micelles using thiol–maleimide coupling reactions.[10] An enhanced micelle uptake by human umbilical vein endothelial cells expressing CD105 *in vitro* and a higher tumor accumulation when compared with the nontargeted micelles *in vivo* were observed.[10] Another example is the anti-intercellular adhesion molecule 1 (ICAM-1) antibody (Ab) conjugated to I-125-radiolabeled gold nanorods through 1-ethyl-3-(3-(dimethylamino)propyl)carbodiimide hydrochloride and *N*-hydroxysulfosuccinimide (EDC/NHS) chemistry.[11] The resulting gold nanorods successfully targeted the inflamed ankle joints in an arthritic rat model where higher levels of ICAM-1 were observed.[11] Furthermore, antiepidermal growth factor receptor (EGFR) Ab has been conjugated to quantum dots through a copper-free "click" reaction.[12] The "click"-conjugated

* Address correspondence to fcaruso@unimelb.edu.au.

Received for review December 5, 2014 and accepted February 15, 2015.

Published online February 25, 2015
10.1021/nn506929e

Ab−quantum dots demonstrated a higher binding affinity to EGFR-positive BxPc-3 and MDA-MB-231 cancer cells when compared with Ab−quantum dots prepared using traditional strategies, which is consistent with the observed internalization characteristics of the respective cell lines.[12]

Although efficient surface functionalization of particles with targeting molecules can be readily achieved by various coupling chemistries, the adsorption of biomolecules (*e.g.*, proteins) onto particles in biological media causes further surface modification.[13] Many particulate systems adsorb proteins when introduced into biological fluids (*e.g.*, interstitial fluid, plasma, and lymph), forming a "protein corona".[13,14] It is widely acknowledged that the protein corona significantly alters the properties of particles, thereby determining the biological identity of the particles.[13−15] For example, the formation of a protein corona around citrate-functionalized silver nanoparticles can stabilize the particles by changing their agglomeration kinetics.[16] Furthermore, the protein corona derived from human plasma on silica and polystyrene nanoparticles can prevent hemolysis of bare nanoparticles and inhibit activation of thrombocytes.[17] In the context of targeted interactions, the deposition of proteins on bicyclononyne-functionalized silica nanoparticles shielded alkyne groups toward coupling with azide groups on a planar silicon substrate.[18] Additionally, the formation of protein coronas in cell culture media containing serum results in significant losses in the specificity of transferrin-functionalized silica nanoparticles.[19] Similarly, a considerable reduction in the targeting ability of single-domain Ab (sdAb)-functionalized silica nanoparticles in serum-containing media was observed.[20] These studies highlight the important roles of protein coronas in controlling the surface properties of nanoparticles. Because the formation of protein coronas is a complex process influenced by many factors, including the physicochemical properties of particles, it is likely that protein coronas influence the particle surface functionality to varying degrees in different particle systems.

In recent years, polymer particles assembled via the layer-by-layer (LbL) technique have emerged as a class of particulate systems that have potential application in advanced drug delivery.[21−23] Owing to its ability to precisely control key physicochemical properties of particles (*e.g.*, size, composition, and surface chemistry) and to load and release cargo on demand, the LbL technique is a powerful tool for designing tailor-made drug delivery systems.[24−26] Furthermore, several generic approaches to functionalize LbL particle surfaces with various macromolecules have been reported, providing a means of enhancing the specificity of particles toward their biological targets.[27−29] As exemplified, humanized A33 (huA33) mAb has been used to functionalize the surface of LbL-assembled poly(*N*-vinylpyrrolidone) (PVPON) capsules through "click" chemistry. These capsules displayed high specific targeting to human A33 positive colon cancer cells, even in the presence of less than 0.1% positive cells in a mixed cell population and a capsule-to-total cell ratio of 0.1:1 in phosphate-buffered saline (PBS) solution.[27] While the huA33 mAb-functionalized capsules have been shown to specifically recognize the cell membrane of A33-expressing cells, the internalization of these huA33 mAb-functionalized capsules is largely *via* macropinocytosis.[30] However, the above-mentioned studies[27−30] have not addressed the effect of protein coronas on the targeting specificity. Additionally, studies have shown that protein adsorption is strongly dependent on the concentration and nature of the biological environment.[31] This finding suggests that the targeting specificity in PBS may bear limited relation to that in more physiologically relevant biological fluids (*e.g.*, blood) owing to the formation of different protein coronas. Therefore, systematic studies on the targeting ability of LbL particles in the presence of protein coronas are required.

Scheme 1. Schematic representation of the assembly of monoclonal antibody-functionalized polymer particles, the formation of protein coronas under biological conditions, and targeting of cancer cells using capsules or particles with a "hard" protein corona formed on their surface.

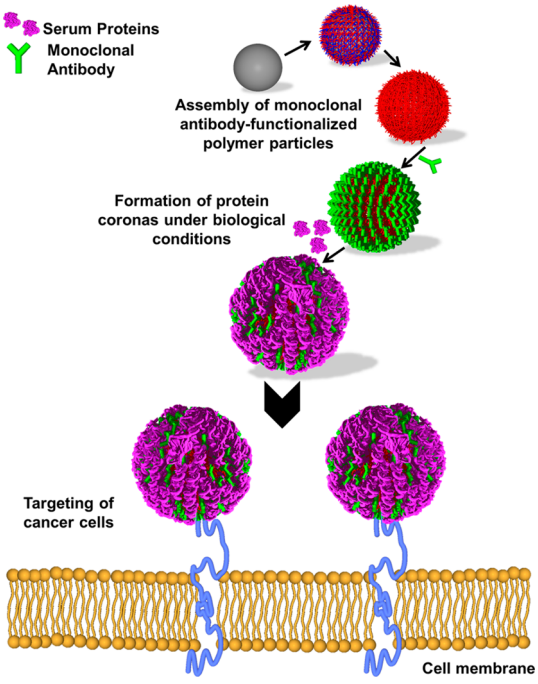

Herein, we investigate the targeting ability of huA33 mAb-functionalized PMA capsules and core−shell particles (referred to as particles in this study) coated with protein coronas derived from human serum at varying concentrations (Scheme 1). The findings show that different concentrations of human serum resulted in different protein compositions in the protein coronas. Incubation with 100% human serum (corresponding to a total protein concentration of approximately

70 mg mL^{-1}) yielded the highest amount of protein adsorbed onto both planar and capsule or particle surfaces. More specifically, 42 proteins (out of 102 proteins) were present in all protein coronas, as determined by mass spectrometry. Despite the formation of different protein coronas, both huA33 mAb-functionalized capsules and particles retained their targeting capability toward A33-antigen-expressing human colon cancer cells *in vitro*. This study highlights that the surface functionality of engineered particles can be retained in the presence of protein coronas.

RESULTS AND DISCUSSION

HuA33 mAb-functionalized PMA capsules and particles with diameters of approximately 2 μm were prepared *via* LbL assembly and functionalized through "click" chemistry, as described previously.[25,27] To confirm the conjugation of the antibodies to the polymer shell of the capsules or particles, huA33 mAbs and PMA were labeled with Alexa Fluor (AF) 488 and 633, respectively. AF488-huA33 mAbs and AF633-PMA were observed by fluorescence microscopy (Figure 1A and C). Transmission electron microscopy (TEM) images showed that the capsules featured many folds and creases and were slightly larger than the particles (Figure 1B and D). By measuring the fluorescence intensity of the AF488-huA33 mAb solution before and after Ab conjugation using fluorescence spectrophotometry, the amount of huA33 mAbs conjugated to 1.6×10^8 capsules or particles was determined (Figure S2). Accordingly, the calculated surface coverage values were $(7.5 \pm 0.7) \times 10^4$ Abs per capsule and $(3.2 \pm 0.5) \times 10^4$ Abs per particle (Figure S2). Based on the dimensions of immunoglobulin G (IgG) determined from X-ray crystallography,[32,33] the theoretically calculated close packing coverage value of Abs ranges from 9.0×10^4 to 1.8×10^5 Abs per particle, depending on their orientation (a hard-sphere model was employed for both capsule and particle systems with diameters of ~2 μm). This finding suggests that the surfaces of both the capsules and particles were not fully saturated by the Abs. The calculated surface coverage values of Abs on the PMA polymer layers was $(6.0 \pm 0.6) \times 10^3$ Abs mm^{-2} for the PMA capsules and $(2.6 \pm 0.4) \times 10^3$ Abs mm^{-2} for the PMA particles, assuming that the polymer layers on the capsules and particles featured the same porosity. The calculated surface coverage values are considerably lower than that obtained for huA33 mAb-functionalized PVPON capsules (approximately $(3.5 \pm 2) \times 10^4$ Abs mm^{-2}) using excess antibodies *via* the "click" coupling approach.[27] The lower coverage observed for the huA33 mAb-PMA capsules was unexpected because the degree of alkyne modification of PMA (~11%) was higher than that of PVPON (~1%). Because the linker and Ab used in both types of capsules were the same, the discrepancy in the surface coverage values suggests that the accessibility of the alkyne groups on the PMA and PVPON capsule surfaces is different, possibly owing to the different local configurations of the polymers.

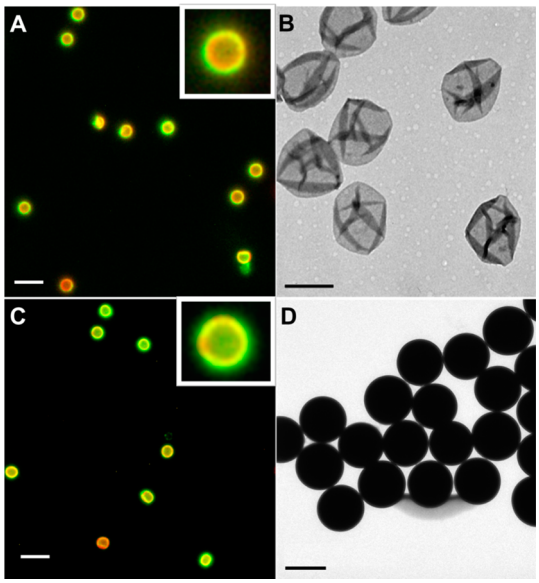

Figure 1. Fluorescence microscopy images (A, C: scale bars are 5 μm) and transmission electron microscopy (TEM) images (B, D: scale bars are 1 μm) of AF633-labeled (red) PMA capsules (A, B) and particles (C, D) functionalized with AF488-labeled huA33 mAbs (green).

To induce the formation of protein coronas, the huA33 mAb-functionalized capsules and particles were incubated in human serum of varying concentrations (0, 10, 50, and 100% (v/v)) in Roswell Park Memorial Institute (RPMI) 1640 medium. The physiochemical properties of the resulting capsules and particles were characterized by dynamic light scattering (DLS). The formation of protein coronas resulted in a slight decrease in the ζ-potential of both the capsules and particles. Specifically, the ζ-potential of the huA33 mAb-functionalized capsules changed from -34 ± 2 (in the absence of a protein corona) to -29 ± 1 (10% serum), -25 ± 4 (50% serum), and -24 ± 2 mV (100% serum). Similarly, a change in the ζ-potential of the huA33 mAb-functionalized particles was observed, *i.e.*, from -39 ± 4 (in the absence of a protein corona) to -33 ± 2 (10% serum), -28 ± 2 (50% serum), and -27 ± 1 mV (100% serum). The results are consistent with the findings of previous studies, which reported that the formation of protein coronas results in neutralization of the surface charge for both positively charged[34,35] and negatively charged nanoparticles.[15,36] Furthermore, atomic force microscopy (AFM) was employed to examine the surface morphology of the capsules in the presence and absence of a protein corona. Upon formation of a protein corona, the surface of the capsules was smoother, reflecting the adsorption of proteins onto the surface (Figure 2).

To analyze protein adsorption onto the capsules and particles, equivalent numbers of capsules and particles

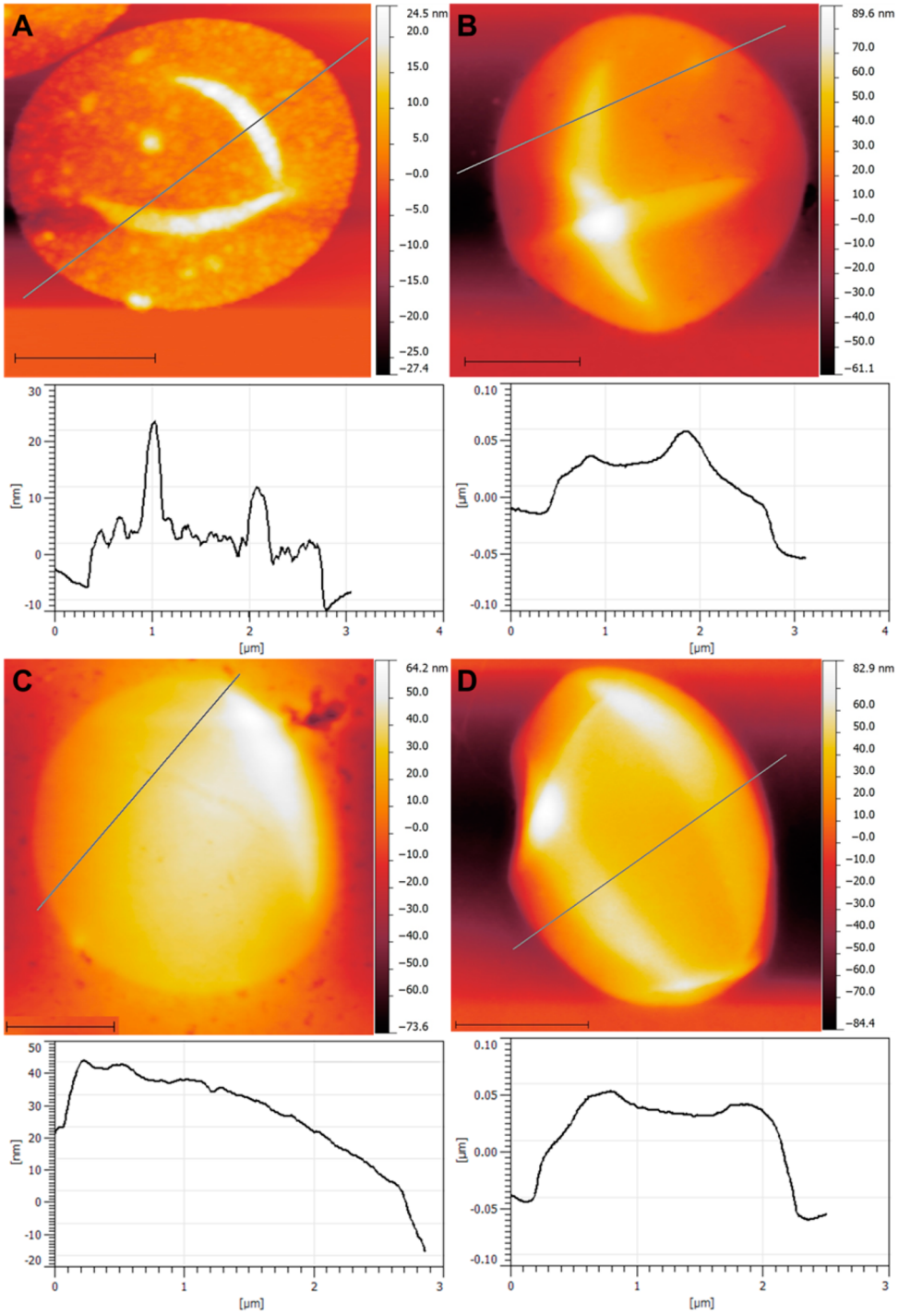

Figure 2. Atomic force microscopy (AFM) images of huA33 mAb-functionalized PMA capsules in the absence (A) and presence (B, C, and D) of a protein corona. Protein coronas were formed in RPMI1640 medium containing 10% (B), 50% (C), or 100% (D) human serum followed by extensive washing with PBS buffer and ultrapure water. The AFM images were taken on air-dried capsules. The associated height profiles of the cross-section of each image are also shown. Scale bars are 1 μm.

functionalized with huA33 mAb or human IgG (huIgG) were exposed to cell media containing human serum at different concentrations. Then, the capsules and particles were extensively washed with PBS buffer to obtain "hard" protein coronas (a relatively stable layer of proteins coated on the capsule or particle surface). This procedure was used as a standard to obtain protein corona-coated polymer capsules and particles in this study. Subsequently, these proteins were eluted and analyzed by sodium dodecyl sulfate-polyacrylamide gel electrophoresis (SDS-PAGE) (Figure 3). As observed, proteins, in particular those with molecular weights above 25 kDa, adsorbed onto all capsule and particle surfaces. On the basis of the density of the bands in each

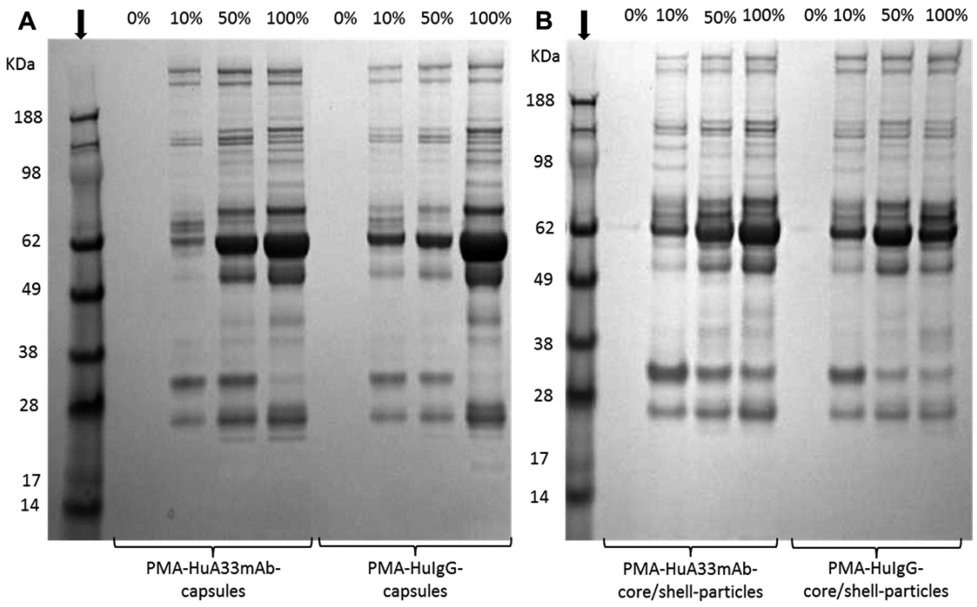

Figure 3. Sodium dodecyl sulfate-polyacrylamide gel electrophoresis (SDS-PAGE) images of separated corona proteins of the huA33 mAb- or huIgG-functionalized PMA capsules (A) or particles (B) following incubation for 1 h at 4 °C in RPMI1640 medium containing human serum at varying concentrations (0, 10, 50, 100% (v/v)). Reference bands associated with particular molecular weights are displayed in each image (as indicated by an arrow).

lane, higher serum concentrations led to increased total protein adsorption (Figure 3). Quartz crystal microbalance with dissipation (QCM-D) analysis also showed that the amount of serum-derived proteins adsorbed onto huA33 mAb-functionalized PMA films increased with higher concentrations of serum (Figure S3). Likewise, polystyrene nanoparticles demonstrated an increase in the amount of proteins adsorbed with increasing plasma concentrations.[31] In contrast, lower amounts of proteins adsorbed onto silica nanoparticles were observed in highly concentrated plasma.[31] This finding suggests that protein adsorption is influenced by other factors such as particle properties (*e.g.*, surface charge, hydrophobicity) besides protein concentration.

To quantitatively analyze the protein composition, mass spectrometry was employed. This method allows direct comparison of the protein compositions in different coronas. Following removal of excess unbound proteins by extensive washing with PBS, the "hard" corona proteins were eluted, reduced, and labeled with formaldehyde containing various isotopes. A total of 83 proteins were identified in the capsule corona derived from 100% human serum, 73 proteins of which were also found in the capsule corona derived from 10% serum. A total of 65 proteins were identified in the particle corona derived from 100% human serum, 60 proteins of which were present in the particle corona derived from 10% serum (Tables S1 and S2). For both particle and capsule coronas, most of the proteins were more abundant in the 100% human serum-derived coronas when compared with those in the 10% human serum-derived coronas. Conversely, the concentration of complement C1q protein subunits was higher in the 10% human serum-derived coronas when compared with that in the 100% human serum-derived coronas for both the capsules and particles. This result indicates that the composition of the protein corona is different for the coronas derived from 10% and 100% human serum.

To verify if the targeting properties of the functionalized capsules and particles was maintained in the presence of a protein corona, the specific binding of the Ab-functionalized capsules and particles to the targeted cells was evaluated using a mixed cell population comprising LIM2405+ and LIM2405− cells at a ratio of 1:1. LIM2405+ cells were derived from a clone that was stably transfected to express A33 on the cell surface membrane. LIM2405− cells, which correspond to a clone that was stably transfected with a control vector, were used as a control; hence, they remain as A33-negative cells. Equivalent numbers of protein corona-coated capsules and particles were incubated with LIM2405+/− cell mixtures in a serum-free medium at 4 °C to prevent cell internalization. Flow cytometry was used to quantitatively measure the binding degree of the capsules and particles to each cell type in the cell mixtures (Figure 4). In the absence of protein coronas, a significantly higher percentage of LIM2405+ cells bound to the Ab-functionalized capsules (66.8%) and particles (90.5%) when compared with the LIM2405− cells (1.5% and 4.6% for the capsules and particles, respectively). These results suggest a high degree of cell recognition driven by antibody-specific interactions (Figure 4). The Ab-functionalized capsules and particles with different protein coronas formed in human serum at varying concentrations were

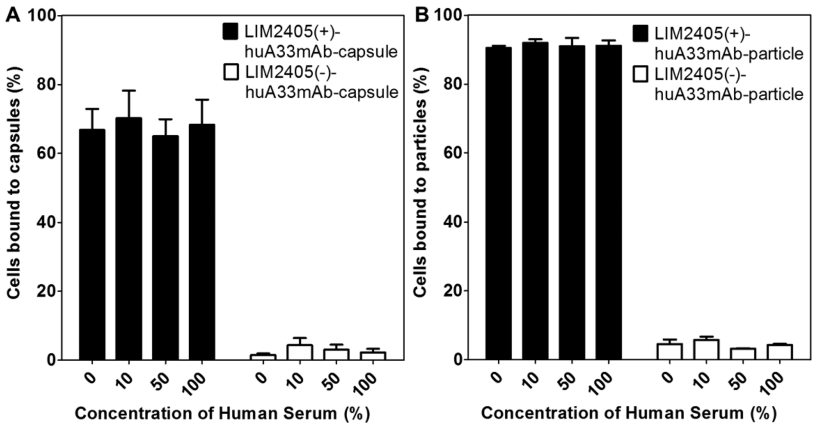

Figure 4. Cell membrane binding of the AF633-labeled PMA capsules and particles to LIM2405+/− cell mixtures (positive-to-negative cell ratio of 1:1) in the presence of protein coronas. Mixed cells were incubated with capsules (A) or particles (B) at 4 °C for 1 h at a capsule- or particle-to-positive cell ratio of 100:1 in a serum-free medium. The percentage of cells bound to the capsules or particles was determined by flow cytometry. Data are shown as the mean ± standard error of at least three independent experiments, with at least 10 000 cells analyzed in each experiment.

separately incubated with the LIM2405+/− cell mixtures. The different corona-coated capsules and particles all exhibited unchanged targeting capacity for LIM2405+ cells in the mixed cell population. Specifically, in the presence of 10% serum-derived coronas, 70.3% and 91.9% of LIM2405+ cells bound to the capsules and particles, respectively. In the presence of 50% serum-derived coronas, 65.1% and 91.0% of LIM2405+ cells were targeted by the capsules and particles, respectively. Furthermore, in the presence of coronas derived from 100% serum, 68.3% and 91.1% of LIM2405+ cells associated with the capsules and particles, respectively (Figure 4). Also, it is noted that the formation of protein coronas did not significantly alter the nonspecific binding to the control LIM2405− cells; the corona-coated capsules and particles obtained in different human serum concentrations displayed cell membrane binding capacities of 4.4% and 5.8% (10% serum), 3.1% and 3.2% (50% serum), 2.3% and 4.3% (100% serum), respectively (Figure 4). These results suggest that the huA33 mAb molecules on the capsules and particles are accessible to the A33 protein on the cell membrane in the presence of the protein coronas. Deconvolution microscopy was employed to confirm the targeting ability of the capsules and particles in the presence of protein coronas. The capsules and particles coated with protein coronas derived from 100% human serum both showed enhanced affinity to targeted LIM2405+ cells (blue) compared with the control LIM2405− cells (green) (Figure 5B and D). The observed enhanced affinity to the targeted LIM2405+ cells was similar to the selectivity of the capsules and particles obtained in the LIM2405+/− cell mixtures in the absence of a protein corona (Figure 5A and C).

To further confirm that the unchanged targeting ability is not specific to one cell line, another A33-positive human colon cancer cell line, LIM1899, was used to investigate the cell membrane binding. HuIgG-functionalized capsules and particles were used as a

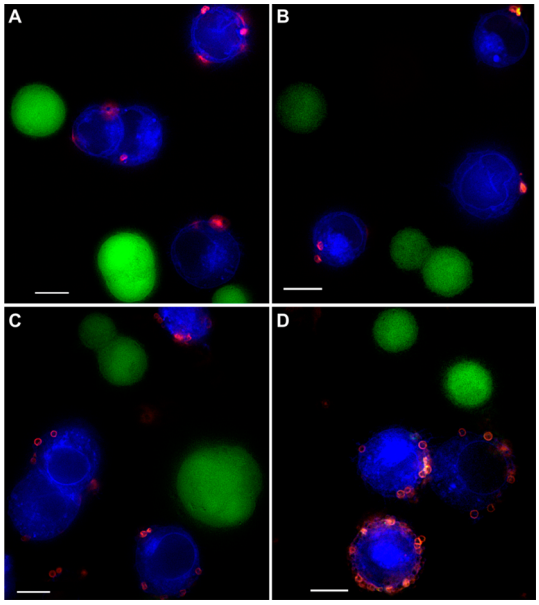

Figure 5. Deconvolution microscopy images of LIM2405+ cells and LIM2405− cells incubated with the huA33 mAb-functionalized PMA capsules (A, B) or particles (C, D) in the absence (A, C) or presence (B, D) of a protein corona. The protein corona was derived from 100% human serum. Mixed cells were incubated with the capsules or particles at 4 °C for 1 h at a capsule- or particle-to-positive cell ratio of 100:1 in a serum-free medium. Cells were imaged using deconvolution microscopy in DPBS. LIM2405+ cells were stained with DiI and pseudocolored blue. LIM2405− cells were stained with CellTracker Green CMFDA, colored green. The particles were labeled with both AF488 (labeled to huA33 mAbs) and AF633 (labeled to PMA). Scale bars are 10 μm.

negative control to show nonspecific cell binding background of the functionalized capsules and particles. "Hard" protein corona-coated capsules and particles functionalized with either huA33 mAb or huIgG were obtained using the same process mentioned earlier. LIM1899 cells were incubated in the presence of the protein corona-coated capsules or particles in a

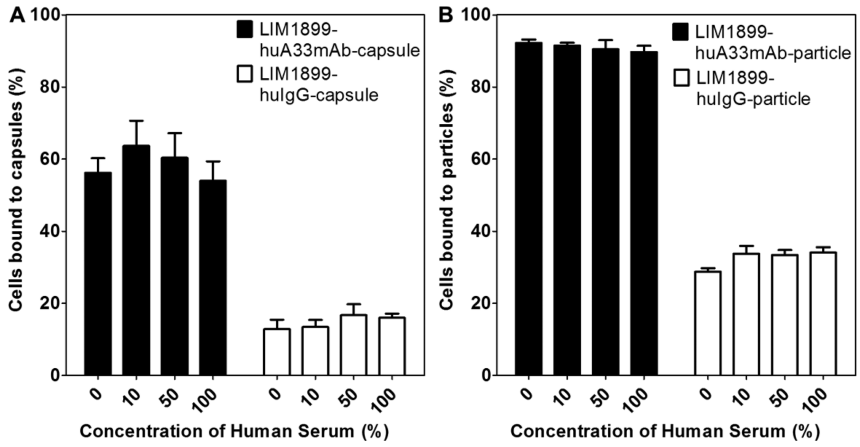

Figure 6. Cell membrane binding of the AF633-labeled PMA capsules and particles to LIM1899 cells in the presence of protein coronas. Mixed cells were incubated with capsules (A) or particles (B) at 4 °C for 1 h at a capsule- or particle-to-cell ratio of 100:1 in a serum-free medium. The percentage of cells bound to the capsules or particles was determined by flow cytometry. Data are shown as the mean ± standard error of at least three independent experiments, with at least 10 000 cells analyzed in each experiment.

serum-free medium at 4 °C to prevent cell internalization. Flow cytometry was used to quantitatively measure the binding degree of the capsules and particles (Figure 6). The targeting effect was evaluated by comparing the amounts of cells that bound to the huA33 mAb- and huIgG-functionalized capsules or particles. The data showed that in both the absence and presence of protein coronas the huA33 mAb-functionalized capsules or particles consistently exhibited enhanced cell membrane binding relative to the control huIgG-functionalized capsules or particles (Figure 6). Specifically, the increased cell binding values (calculated as the difference between the percentage of cells bound to the huA33 mAb-functionalized capsules or particles and the percentage of cells bound to the huIgG-functionalized carriers) obtained for the functionalized capsules and particles were respectively 43% and 63% (0% serum), 50% and 58% (10% serum), 44% and 57% (50% serum), and 38% and 56% (100% serum) (Figure 6). The comparable cell binding values obtained in the presence of different protein coronas and absence of a protein corona suggest that the targeting ability of such huA33 mAb-functionalized capsules and particles was unchanged in the presence of a protein corona.

Cell membrane targeting experiments using LIM1899 and LIM2405 cell lines both exhibited the same result: the targeting ability of the huA33 mAb-functionalized PMA capsules and particles was retained in the presence of a "hard" protein corona layer formed on the capsules' and particles' surfaces. This indicates that, despite the surface coating on the polymer capsules or particles, the layer of a "hard" protein corona does not reduce the ability of huA33 mAbs to recognize A33 proteins on the cell surface. Previous studies have shown that transferrin- or sdAb-functionalized silica nanoparticles completely or partially lose their targeting specificity in the presence of protein coronas.[19,20] The discrepancy observed in the effect of protein coronas on targeting could possibly be explained as follows. First, different binding affinities to the corresponding receptors or antigens on the cell membrane may exist across different carriers. In general, the equilibrium dissociation constant (K_D) for monoclonal antibodies and antigens is on the order of pM and nM−pM for sdAbs and antigens and nM for transferrin and transferrin receptors. However, the affinity of these targeting molecules on different particles remains unclear considering that affinity can be enhanced *via* multivalency on the particle surface, which is likely to be dependent on the ligand density. With a higher affinity, antibodies tend to be less affected than other proteins in achieving their targeting ability in biological environments. Second, the molecular sizes of the targeting moieties employed in these studies were different. Generally, an Ab (~150 kDa) is larger than a transferrin (~80 kDa) or a sdAb (~15 kDa). The larger size of Ab may prevent complete shielding of the molecules on the particle surface, thereby favoring preservation of the capsule or particle targeting ability.

CONCLUSION

The present study examined the formation of protein coronas on huA33 mAb-functionalized LbL-assembled PMA capsules and core−shell particles and the effects of protein coronas on the surface functionality of such carriers. The findings showed that the composition of the protein coronas differed between the capsules and particles and was additionally influenced by the concentration of serum in biological media. Consistent with other studies, the formation of protein coronas led to changes in the ζ-potential and roughness of the capsules. To examine the effects of protein coronas on the targeting ability of the capsules and particles, two stably transfected cell lines were employed (LIM2405+ cells expressing A33 and LIM2405− cells lacking A33 expression). As observed, huA33 mAb functionalization enhanced the cell

membrane binding of the capsules and particles toward LIM2405+ cells; this enhanced affinity remained unaltered in the presence of the protein coronas formed. Moreover, comparison of the cell membrane binding of the huA33 mAb- and huIgG-functionalized capsules and particles toward the A33-expressing cells confirmed that the specific binding driven by huA33 mAb-A33 interactions remained the same in either the absence or presence of the protein coronas. In summary, our data demonstrate that the adsorption of a "hard" protein corona layer onto the surface of soft polymeric capsules or particles is not detrimental to the ability of huA33 mAbs to recognize A33 proteins on the cell membrane. Owing to the importance of protein coronas in directing the surface properties of particles, this study indicates that antibody specificity can be retained in the presence of protein coronas.

METHODS

Materials. Poly(methacrylic acid) (PMA, M_w 15 kDa) was purchased from Polysciences (Warrington, PA, USA). SiO_2 particles were purchased from Micro Particles GmbH (Berlin, Germany). Hydrofluoric acid (HF), ammonium fluoride (NH_4F), sodium acetate (NaOAc), sodium bicarbonate, poly(*N*-vinylpyrrolidone) (PVPON; M_w ~10 kDa), sodium ascorbate, copper sulfate, phosphate-buffered saline (PBS) tablets, polyethylenimine (PEI), 1-ethyl-3-(3-(dimethylamino)propyl) carbodiimide (EDC), dimethyl sulfoxide (DMSO), propargylamine hydrochloride, deuterium oxide, and 4-(4,6-dimethoxy-1,3,5-triazin-2-yl)-4-methylmorpholin-4-ium (DMTMM) were purchased from Sigma–Aldrich (Sydney, Australia) and used as received. Alexa Fluor 633 hydrazide and Alexa Fluor 488 succinimidyl ester reactive dyes, RPMI1640 medium containing L-glutamine (300 mg L^{-1}), fetal bovine serum (FBS), Dulbecco phosphate-buffered saline (DPBS), NuPAGE Bis-Tris precast gel 4–12%, NuPAGE MES SDS running buffer, NuPAGE LDS sample buffer, NuPAGE sample reducing agent, human immunoglobulin (huIgG), CellTracker Green CMFDA (5-chloromethyl fluorescein diacetate), and G418 sulfate (50 mg mL^{-1}) used for LIM2405 cell culture were purchased from Life Technologies (Mulgrave, Victoria, Australia). Succinimidyl ester and azide-bifunctionalized poly(ethylene glycol) (NHS-PEG-Az) was purchased from JenKem Technologies (USA). Ultrapure water with a resistance greater than 18 MΩ cm was obtained from an inline Millipore RiOs/Origin system (Millipore Corporation, USA). HuA33 mAbs and LIM1899 and LIM2405 cell lines were provided by Prof. Andrew Scott at the Ludwig Institute for Cancer Research, Austin Hospital, Melbourne, Australia.

Layer-by-Layer Polymer Particle Preparation. The synthesis of alkyne-functionalized poly(methacrylic acid) (PMA-Alk; alkyne functionalization degree ~11%) is described in the Supporting Information. The synthesis of the disulfide reducible crosslinker *N*,*N*′-(dithiodiethane-2,1-diyl)bis(1-azido tetraethylene glycol acetamide) and subsequent LbL assembly of the degradable capsules and particles were outlined previously.[25,27] A standard washing procedure was employed as follows: a 200 μL SiO_2 particle suspension (50 mg mL^{-1}; diameter 1.16 μm) was centrifuged at 1000*g* for 60 s. The supernatant was removed, and the particles were dispersed in 1000 μL of NaOAc buffer (pH 4, 50 mM). Three centrifugation/redispersion cycles were conducted. Following washing, 1000 μL of PVPON (1 mg mL^{-1}) in NaOAc buffer (pH 4, 50 mM) was added to the particles for adsorption onto the silica surface for 15 min with constant shaking. The resulting particles were washed using the standard washing procedure described above. Then, to adsorb a PMA-Alk layer onto the PVPON layer, 1000 μL of PMA-Alk (1 mg mL^{-1}) prepared in NaOAc buffer (pH 4, 50 mM) was used with constant shaking for 15 min. The particles were then washed to create a PVPON/PMA-Alk bilayer. The PVPON/PMA-Alk bilayer adsorption process was repeated four more times. The multilayer shell was covalently cross-linked by incubating the particles with a 1500 μL solution containing the "click" crosslinker (1 mg mL^{-1}), sodium ascorbate (4.4 mg mL^{-1}), and copper sulfate (1.8 mg mL^{-1}) at a v/v/v ratio of 3:1:1 in NaOAc buffer (pH 4, 50 mM) for 12 h with constant shaking. The cross-linked particles were then washed three times with NaOAc buffer (pH 4, 50 mM).

The capsules were formed by dissolving the silica templates using NH_4F (13.3 M)-buffered HF (5 M) at pH 4. (*Caution! HF is highly toxic and great care must be taken during handling*). The capsules were centrifuged (3800*g*, 8 min) and washed three times using NaOAc buffer (pH 4, 50 mM). To remove the hydrogen-bonded PVPON from the cross-linked multilayers, the capsules or particles were incubated in PBS buffer at pH 7.4 for approximately 12 h.

Fluorescent Labeling of Capsules and Particles. First, 500 μL of EDC (10 mg mL^{-1}) prepared in PBS buffer at pH 7.4 was mixed with 500 μL of five-layered capsule or particle suspensions in PBS. Subsequently, 5 μL of AF633-hydrazide (1 mg mL^{-1}) in dry DMSO was added to the mixture. Samples were incubated in the dark with constant shaking for 16 h at ~22 °C. After labeling, the capsules and particles were washed three times in PBS and counted using flow cytometry (Apogee Flow) to determine their concentration.

Ab-Conjugation to Capsules and Particles. First, 5 μg of Ab–Az was added to 1.6×10^8 PMA capsules or particles in PBS containing 10 μL of sodium ascorbate (4.4 mg mL^{-1}), 10 μL of copper(II) sulfate (1.8 mg mL^{-1}), and 10 μL of chelator (tris[(4-carboxyl-1-benzyl-1*H*-1,2,3-triazol-4-yl)methyl]amine, TCBTMA; 4.89 mg mL^{-1}). The samples were incubated with constant shaking for 1 h at 4 °C. After functionalization, the capsules or particles were washed twice in PBS buffer and counted using flow cytometry (Apogee Flow) to determine their concentration.

Formation of Protein Corona-Coated Capsules and Particles. huIgG- or huA33 mAb-functionalized capsules or particles (1×10^8) were incubated in 1 mL of human serum at varying concentrations in RPMI1640 media (0, 10, 50, and 100% (v/v)) for 1 h at 4 °C. The capsules or particles were then washed three times with PBS buffer to obtain the "hard" protein corona-coated capsules or particles. These "hard" protein corona-coated capsules and particles were used directly for cell-binding and proteomic experiments or further washed with different buffers or ultrapure water for characterization.

Characterization of Polymer Particles. After formation of protein coronas, the capsules and particles were isolated and characterized by the following methods. Differential interference contrast (DIC) and fluorescence microscopy images were taken with an inverted Olympus IX71 microscope. Atomic force microscopy experiments were conducted on an Asylum Research AFM. Typical scans were conducted in tapping mode using MikroMasch silicon cantilevers (NSC/CSC). The film thickness and roughness of the polymer capsules were analyzed using an SPM data visualization and analysis tool, Gwyddion version 2.34. Transmission electron microscopy images were acquired on a FEI Tecnai TF20 instrument, operating at 200 kV. Prior to TEM analysis, the samples (1 μL) were dropped onto Formvar-coated copper grids and allowed to air-dry. Microelectrophoresis (Zeta Sizer 2000, Malvern Instruments) was employed to measure the ζ-potential of huA33 mAb-functionalized PMA capsules and particles in phosphate buffer (pH 7.2, 5 mM).

Sodium Dodecyl Sulfate-Polyacrylamide Gel Electrophoresis. For the analysis, 1×10^8 huIgG- or huA33 mAb-functionalized capsules or particles were incubated in 1 mL of human serum at varying concentrations in RPMI1640 media (0, 10, 50, and 100% (v/v)) for 1 h at 4 °C. The capsules or particles were then washed three times with DPBS buffer to obtain the protein corona-coated

capsules or particles. The adsorbed proteins were stripped from the capsules or particles by adding NuPAGE LDS sample loading buffer and heated at 70 °C for 10 min. The eluted proteins were transferred to a new tube. The disulfide bonds in proteins were cleaved using a reducing agent (50 mM dithiothreitol) and heated at 70 °C for 10 min. The samples were then loaded on the gel and run for ~50 min at 200 V. Each gel included one lane of a standard molecular weight ladder.

Cell Culture. Human colorectal cancer cell lines LIM1899, LIM2405+, and LIM2405− were cultured in RPMI1640 medium containing 10% FBS, 0.6 mg mL^{-1} G418 sulfate (for LIM2405 cell lines only), and other supplements (10.8 μg mL^{-1} α-thioglycerol, 0.025 U mL^{-1} insulin, and 1 μg mL^{-1} hydrocortisone) at 37 °C in a 5% CO_2-humidified atmosphere and subcultured prior to confluence.

Flow Cytometry Involving the LIM1899 Cell Line. First, 1×10^7 huIgG- or huA33 mAb-functionalized capsules or particles coated with protein coronas were added to 1×10^5 LIM1899 cells (the particle-to-LIM1899 cell ratio was 100:1) in 500 μL of serum-free RPMI1640 medium. The cells were incubated with the capsules or particles for 1 h at 4 °C followed by three washes with cold DPBS buffer. The cell pellets were resuspended in 300 μL of DPBS buffer and analyzed by flow cytometry (Apogee Flow). Analysis was performed using FlowJo vX.0.6. Cells that displayed 638-Red (AF633) signals above 100 were identified as those associated with the capsules or particles.

Flow Cytometry Involving the LIM2405 Cell Line (A33-Antigen Positive and Negative Cell Mixture). LIM2405− cells were stained with 2 μM CellTracker Green CMFDA for the flow cytometry measurements. A 50:50 mixture of LIM2405− and LIM2405+ (total of 2×10^5 cells) was prepared, to which the huIgG- or huA33 mAb-functionalized capsules or particles coated with protein coronas were added (particle-to-LIM2405+ cell ratio was 100:1). The cells were incubated with the capsules or particles in 500 μL of serum-free RPMI1640 medium for 1 h at 4 °C followed by three washes with cold DPBS buffer. The cell pellets were resuspended in 300 μL of DPBS buffer and analyzed by flow cytometry (Apogee Flow). Analysis was performed using FlowJo vX.0.6. The LIM2405+ and LIM2405− cells were identified according to their cell tracker staining. Cells that displayed 638-Red (AF633) signals above 100 were identified as those associated with the capsules or particles.

Deconvolution Fluorescence Microscopy. For the deconvolution microscopy analysis, the LIM2405− cells were stained with 3 μM CellTracker Green CMFDA and the LIM2405+ cells were stained with 1,1′-dioctadecyl-3,3,3′,3′-tetramethylindocarbocyanine perchlorate (DiI, 4 μM). The capsules and particles coated with protein coronas were prepared following the protocols mentioned above. Cell membrane binding experiments were performed following the same protocols mentioned above. Deconvolution fluorescence microscopy was performed on a DeltaVision (Applied Precision) microscope with a 60× 1.516 NA oil objective and a standard FITC/TRITC/CY5 filter set. Images were processed with Imaris (Bitplane) using the maximum intensity projection unless otherwise noted.

Conflict of Interest: The authors declare no competing financial interest.

Supporting Information Available: Experimental details for the preparation of polymer and antibodies, QCM-D measurements, and mass spectrometry-dimethyl labeling; results for Ab-adsorption experiments, QCM-D measurements, and mass spectrometry. This material is available free of charge *via* the Internet at http://pubs.acs.org.

Acknowledgment. This work was supported by the Australian Research Council under the Australian Laureate Fellowship (F.C., FL120100030), Discovery Early Career Researcher Award (Y.Y., DE130100488), and the Australian Research Council Centre of Excellence in Convergent Bio-Nano Science and Technology (project number CE140100036) schemes, as well as the Feodor-Lynen Fellowship from the Alexander von Humboldt Foundation (K.K.). Q.D. acknowledges funding from the Australian Government through an International Postgraduate Research Scholarship and an Australian Postgraduate Award. We acknowledge Ms. Marta Redrado Notivoli (platform support officer—colloidal characterization from The Melbourne Materials Institute) for assistance with acquisition of AFM images, Dr. Huanli Sun for assistance with NMR measurement and analysis, and Mr. Junling Guo for assistance with acquisition of TEM images.

REFERENCES AND NOTES

1. Accardo, A.; Tesauro, D.; Morelli, G. Peptide-Based Targeting Strategies for Simultaneous Imaging and Therapy with Nanovectors. *Polym. J.* **2013**, *45*, 481–493.
2. Schroeder, A.; Heller, D. A.; Winslow, M. M.; Dahlman, J. E.; Pratt, G. W.; Langer, R.; Jacks, T.; Anderson, D. G. Treating Metastatic Cancer with Nanotechnology. *Nat. Rev. Cancer* **2012**, *12*, 39–50.
3. Rajendran, L.; Knolker, H. J.; Simons, K. Subcellular Targeting Strategies for Drug Design and Delivery. *Nat. Rev. Drug Discovery* **2010**, *9*, 29–42.
4. Yan, Y.; Such, G. K.; Johnston, A. P. R.; Best, J. P.; Caruso, F. Engineering Particles for Therapeutic Delivery: Prospects and Challenges. *ACS Nano* **2012**, *6*, 3663–3669.
5. Xia, W.; Low, P. S. Folate-Targeted Therapies for Cancer. *J. Med. Chem.* **2010**, *53*, 6811–6824.
6. Daniels, T. R.; Bernabeu, E.; Rodriguez, J. A.; Patel, S.; Kozman, M.; Chiappetta, D. A.; Holler, E.; Ljubimova, J. Y.; Helguera, G.; Penichet, M. L. The Transferrin Receptor and the Targeted Delivery of Therapeutic Agents against Cancer. *Biochim. Biophys. Acta, Gen. Subj.* **2012**, *1820*, 291–317.
7. Cerchia, L.; de Franciscis, V. Targeting Cancer Cells with Nucleic Acid Aptamers. *Trends Biotechnol.* **2010**, *28*, 517–525.
8. Svensen, N.; Walton, J. G. A.; Bradley, M. Peptides for Cell-Selective Drug Delivery. *Trends Pharmacol. Sci.* **2012**, *33*, 186–192.
9. Weiner, L. M.; Surana, R.; Wang, S. Z. Monoclonal Antibodies: Versatile Platforms for Cancer Immunotherapy. *Nat. Rev. Immunol.* **2010**, *10*, 317–327.
10. Guo, J. T.; Hong, H.; Chen, G. J.; Shi, S. X.; Zheng, Q. F.; Zhang, Y.; Theuer, C. P.; Barnhart, T. E.; Cai, W. B.; Gong, S. Q. Image-Guided and Tumor-Targeted Drug Delivery with Radiolabeled Unimolecular Micelles. *Biomaterials* **2013**, *34*, 8323–8332.
11. Shao, X.; Zhang, H.; Rajian, J. R.; Chamberland, D. L.; Sherman, P. S.; Quesada, C. A.; Koch, A. E.; Kotov, N. A.; Wang, X. ^{125}I-Labeled Gold Nanorods for Targeted Imaging of Inflammation. *ACS Nano* **2011**, *5*, 8967–8973.
12. Kotagiri, N.; Li, Z.; Xu, X.; Mondal, S.; Nehorai, A.; Achilefu, S. Antibody Quantum Dot Conjugates Developed *via* Copper-Free Click Chemistry for Rapid Analysis of Biological Samples Using a Microfluidic Microsphere Array System. *Bioconjugate Chem.* **2014**, *25*, 1272–1281.
13. Monopoli, M. P.; Aberg, C.; Salvati, A.; Dawson, K. A. Biomolecular Coronas Provide the Biological Identity of Nanosized Materials. *Nat. Nanotechnol.* **2012**, *7*, 779–786.
14. Walkey, C. D.; Chan, W. C. W. Understanding and Controlling the Interaction of Nanomaterials with Proteins in a Physiological Environment. *Chem. Soc. Rev.* **2012**, *41*, 2780–2799.
15. Yan, Y.; Gause, K. T.; Kamphuis, M. M. J.; Ang, C. S.; O'Brien-Simpson, N. M.; Lenzo, J. C.; Reynolds, E. C.; Nice, E. C.; Caruso, F. Differential Roles of the Protein Corona in the Cellular Uptake of Nanoporous Polymer Particles by Monocyte and Macrophage Cell Lines. *ACS Nano* **2013**, *7*, 10960–10970.
16. Gebauer, J. S.; Malissek, M.; Simon, S.; Knauer, S. K.; Maskos, M.; Stauber, R. H.; Peukert, W.; Treuel, L. Impact of the Nanoparticle-Protein Corona on Colloidal Stability and Protein Structure. *Langmuir* **2012**, *28*, 9673–9679.
17. Tenzer, S.; Docter, D.; Kuharev, J.; Musyanovych, A.; Fetz, V.; Hecht, R.; Schlenk, F.; Fischer, D.; Kiouptsi, K.; Reinhardt, C.; *et al*. Rapid Formation of Plasma Protein Corona Critically Affects Nanoparticle Pathophysiology. *Nat. Nanotechnol.* **2013**, *8*, 772–781.
18. Mirshafiee, V.; Mahmoudi, M.; Lou, K. Y.; Cheng, J. J.; Kraft, M. L. Protein Corona Significantly Reduces Active Targeting Yield. *Chem. Commun.* **2013**, *49*, 2557–2559.

19. Salvati, A.; Pitek, A. S.; Monopoli, M. P.; Prapainop, K.; Bombelli, F. B.; Hristov, D. R.; Kelly, P. M.; Aberg, C.; Mahon, E.; Dawson, K. A. Transferrin-Functionalized Nanoparticles Lose Their Targeting Capabilities when a Biomolecule Corona Adsorbs on the Surface. *Nat. Nanotechnol.* **2013**, *8*, 137–143.
20. Zarschler, K.; Prapainop, K.; Mahon, E.; Rocks, L.; Bramini, M.; Kelly, P. M.; Stephan, H.; Dawson, K. A. Diagnostic Nanoparticle Targeting of the EGF-Receptor in Complex Biological Conditions Using Single-Domain Antibodies. *Nanoscale* **2014**, *6*, 6046–6056.
21. Yan, Y.; Björnmalm, M.; Caruso, F. Assembly of Layer-by-Layer Particles and Their Interactions with Biological Systems. *Chem. Mater.* **2014**, *26*, 452–460.
22. Ariga, K.; Yamauchi, Y.; Rydzek, G.; Ji, Q. M.; Yonamine, Y.; Wu, K. C. W.; Hill, J. P. Layer-by-Layer Nanoarchitectonics: Invention, Innovation, and Evolution. *Chem. Lett.* **2014**, *43*, 36–68.
23. Borges, J.; Mano, J. F. Molecular Interactions Driving the Layer-by-Layer Assembly of Multilayers. *Chem. Rev.* **2014**, *114*, 8883–8942.
24. Quinn, J. F.; Johnston, A. P. R.; Such, G. K.; Zelikin, A. N.; Caruso, F. Next Generation, Sequentially Assembled Ultrathin Films: Beyond Electrostatics. *Chem. Soc. Rev.* **2007**, *36*, 707–718.
25. Kinnane, C. R.; Such, G. K.; Antequera-Garcia, G.; Yan, Y.; Dodds, S. J.; Liz-Marzan, L. M.; Caruso, F. Low-Fouling Poly(*N*-vinyl pyrrolidone) Capsules with Engineered Degradable Properties. *Biomacromolecules* **2009**, *10*, 2839–2846.
26. Such, G. K.; Johnston, A. P. R.; Caruso, F. Engineered Hydrogen-Bonded Polymer Multilayers: From Assembly to Biomedical Applications. *Chem. Soc. Rev.* **2011**, *40*, 19–29.
27. Kamphuis, M. M. J.; Johnston, A. P. R.; Such, G. K.; Dam, H. H.; Evans, R. A.; Scott, A. M.; Nice, E. C.; Heath, J. K.; Caruso, F. Targeting of Cancer Cells Using Click-Functionalized Polymer Capsules. *J. Am. Chem. Soc.* **2010**, *132*, 15881–15883.
28. Leung, M. K. M.; Hagemeyer, C. E.; Johnston, A. P. R.; Gonzales, C.; Kamphuis, M. M. J.; Ardipradja, K.; Such, G. K.; Peter, K.; Caruso, F. Bio-Click Chemistry: Enzymatic Functionalization of PEGylated Capsules for Targeting Applications. *Angew. Chem., Int. Ed.* **2012**, *51*, 7132–7136.
29. Shimoni, O.; Postma, A.; Yan, Y.; Scott, A. M.; Heath, J. K.; Nice, E. C.; Zelikin, A. N.; Caruso, F. Macromolecule Functionalization of Disulfide-Bonded Polymer Hydrogel Capsules and Cancer Cell Targeting. *ACS Nano* **2012**, *6*, 1463–1472.
30. Johnston, A. P. R.; Kamphuis, M. M. J.; Such, G. K.; Scott, A. M.; Nice, E. C.; Heath, J. K.; Caruso, F. Targeting Cancer Cells: Controlling the Binding and Internalization of Antibody-Functionalized Capsules. *ACS Nano* **2012**, *6*, 6667–6674.
31. Monopoli, M. P.; Walczyk, D.; Campbell, A.; Elia, G.; Lynch, I.; Bombelli, F. B.; Dawson, K. A. Physical-Chemical Aspects of Protein Corona: Relevance to *in Vitro* and *in Vivo* Biological Impacts of Nanoparticles. *J. Am. Chem. Soc.* **2011**, *133*, 2525–2534.
32. Caruso, F.; Furlong, D. N.; Ariga, K.; Ichinose, I.; Kunitake, T. Characterization of Polyelectrolyte-Protein Multilayer Films by Atomic Force Microscopy, Scanning Electron Microscopy, and Fourier Transform Infrared Reflection-Absorption Spectroscopy. *Langmuir* **1998**, *14*, 4559–4565.
33. Caruso, F.; Rodda, E.; Furlong, D. N. Orientational Aspects of Antibody Immobilization and Immunological Activity on Quartz Crystal Microbalance Electrodes. *J. Colloid Interface Sci.* **1996**, *178*, 104–115.
34. Barran-Berdon, A. L.; Pozzi, D.; Caracciolo, G.; Capriotti, A. L.; Caruso, G.; Cavaliere, C.; Riccioli, A.; Palchetti, S.; Lagana, A. Time Evolution of Nanoparticle-Protein Corona in Human Plasma: Relevance for Targeted Drug Delivery. *Langmuir* **2013**, *29*, 6485–6494.
35. Huhn, D.; Kantner, K.; Geidel, C.; Brandholt, S.; De Cock, I.; Soenen, S. J. H.; Gil, P. R.; Montenegro, J. M.; Braeckmans, K.; Mullen, K.; *et al*. Polymer-Coated Nanoparticles Interacting with Proteins and Cells: Focusing on the Sign of the Net Charge. *ACS Nano* **2013**, *7*, 3253–3263.
36. Jedlovszky-Hajdu, A.; Bombelli, F. B.; Monopoli, M. P.; Tombacz, E.; Dawson, K. A. Surface Coatings Shape the Protein Corona of SPIONs with Relevance to Their Application *in Vivo*. *Langmuir* **2012**, *28*, 14983–14991.